OXFORD GENETICS

SHC-3: a previously unidentified *C. elegans* Shc family member functions in the insulin-like signaling pathway to enhance survival during L1 arrest

Mercedes Di Bernardo,[1,†] Victoria L. León Guerrero,[1,†] Jacob C. Sutoski,[1] William Rod Hardy,[1,2] Lesley T. MacNeil 🔘 [1,3,4,*]

[1]Department of Biochemistry and Biomedical Sciences, McMaster University, 1280 Main St W, Hamilton, ON L8S 4K1, Canada
[2]Present address: Lunenfeld-Tanenbaum Research Institute, Mount Sinai Hospital, Toronto, ON M5G 1X5, Canada
[3]Farncombe Family Digestive Health Research Institute, McMaster University, 1280 Main St W, Hamilton, ON L8S 4K1, Canada
[4]Michael G. DeGroote Institute for Infectious Disease Research, McMaster University, 1280 Main St W, Hamilton, ON L8S 4K1, Canada

*Corresponding author: Department of Biochemistry and Biomedical Sciences, McMaster University, 1280 Main St W, Hamilton, ON L8S 4K1, Canada. Email: macneil@mcmaster.ca
[†]These authors contributed equally.

Shc (Src homologous and collagen) proteins function in many different signaling pathways where they mediate phosphorylation-dependent protein–protein interactions. These proteins are characterized by the presence of two phosphotyrosine-binding domains, an N-terminal PTB and a C-terminal SH2. We describe a previously unrecognized *Caenorhabditis elegans* Shc gene, *shc-3* and characterize its role in stress response. Both *shc-3* and *shc-1* are required for long-term survival in L1 arrest and survival in heat stress, however, they do not act redundantly but rather play distinct roles in these processes. Loss of *shc-3* did not further decrease survival of *daf-16* mutants in L1 arrest, suggesting that like SHC-1, SHC-3 functions in the insulin-like signaling pathway. In the absence of SHC-3, DAF-16 nuclear entry and exit are slowed, suggesting that SHC-3 is required for rapid changes in DAF-16 signaling.

Keywords: *C. elegans*; insulin-like signaling; SHC; adapter protein; L1 arrest; development; heat stress; DAF-16; DAF-2

Introduction

The regulation of protein–protein interactions by phosphorylation allows rapid transmission of signals with tight control over the timing and length of activity. Proteins that bind specific phosphorylated motifs therefore play critical roles in many signaling pathways. Among these proteins are the Shc (Src homologous and collagen) family proteins that are integral to many cellular pathways where they link activated receptors to downstream effectors.

Shc proteins are found in evolutionarily diverse organisms where they regulate a number of different biological processes, including stress response. They have no enzymatic activity but instead function as intracellular signaling scaffolds, regulating signal-dependent complex formation in part through phosphotyrosine-binding (PTB) and SH2 phosphotyrosine-binding domains. The N-terminal PTB domain binds motifs matching the θ-X-N-X-X-pY consensus (θ = large hydrophobic amino acid), and a C-terminal SH2 domain that binds motifs matching the consensus, pY-θ-X-θ. This domain organization is unique to members of the Shc family. The central region, CH1 (collagen homologous), exhibits limited sequence similarity between Shc proteins of different species. In mammalian ShcA, this region contains two conserved YXN motifs that, when phosphorylated, recruit Grb2 (Rozakis-Adcock *et al.* 1992). The first of these motifs, YYN (Y239/240 in hShcA) is conserved in *Drosophila* but absent in *Caenorhabditis elegans* Shc proteins while the second motif (Y317 in hShcA) is absent from both *Drosophila* and *C. elegans* Shc proteins, suggesting that the role of Grb2 in Shc signaling may not be conserved in these species.

Two *shc* genes were previously reported in *C. elegans*, *shc-1* and *shc-2* (Luzi *et al.* 2000). Little is known about the function of *shc-2*, but *shc-1* functions in stress response pathways, including the insulin-like signaling (IIS) and MAPK pathways, to regulate lifespan, pathogen resistance, dauer formation, and oxidative stress resistance (Neumann-Haefelin *et al.* 2008). Via its PTB domain, mammalian ShcA binds activated insulin receptors (IR or IGFR-1). This binding leads to phosphorylation of ShcA, preferentially on Y317, and subsequent recruitment of Grb2; Grb2 in turn recruits SOS and activates the ras/MAPK pathway. While *C. elegans* SHC-1 both promotes MAPK signaling and binds the DAF-2 receptor, this is unlikely to occur via the same mechanism because SHC-1 lacks the conserved Grb2 binding sites. Further, SHC-1 is proposed to act as a negative regulator of DAF-2 but as a positive regulator of JNK-MAPK signaling, suggesting the two roles are independent (Mizuno *et al.* 2008; Neumann-Haefelin *et al.* 2008). SHC-1 acts as a scaffold bridging MEK-1 and MLK-1, promoting the phosphorylation of MEK-1 and subsequent activation of the JNK-like MAPK KGB-1. SHC-1 functions with MEK-1 and MLK-1 to regulate oxidative stress response, heavy metal resistance, dauer entry, and axon regeneration (Mizuno *et al.* 2008; Hisamoto *et al.* 2016; Dogra *et al.* 2022).

While vertebrates have four Shc genes (Shc1/ShcA, Shc2/ShcB, Shc3/ShcC, and Shc4/ShcD), most invertebrates have a single Shc gene that is most similar to ShcA, suggesting that ShcA is the ancestral Shc gene and that this gene family was expanded in the vertebrate lineage. The *C. elegans* genome contains three genes that encode proteins with Shc-like domain structure, SHC-1, SHC-2 (Luzi *et al.* 2000), and a previously uncharacterized gene, K11E4.2, that we have named *shc-3*. Here we report the identification and characterization of K11E4.2/*shc-3*. Animals lacking *shc-3* show reduced survival in L1 arrest and are more sensitive to heat and pathogen exposure. We find that, like SHC-1, SHC-3 acts on the IIS pathway but that the two proteins do not function redundantly but instead play distinct roles in regulating IIS.

Materials and methods

C. elegans strains

C. elegans were propagated by standard methods (Stiernagle 2006). The *shc-3(syb1634)* deletion allele was generated by Suny Biotech by CRISPR/Cas9. This allele produces a 588 bp deletion immediately after the start ATG that removes exons 1–4. This allele was genotyped by PCR with primers cattctcgatggaattctagtg and caaaaaggtttcgactctattttagg. The *shc-3(gk890887)* mutation was recovered from VC40938 and outcrossed eight times to N2. This mutation produces a stop codon in exon 2 that truncates the protein at amino acid Q39. The *shc-3(gk466377)* allele is a point mutation that generates the R145Q amino acid substitution. This allele was recovered from VC40108 and outcrossed eight generations to N2. VC40938, VC40108, *shc-1(ok198)*, CF1038 *daf-16(mu86)*, RAF2181 *daf-2(bch-40[degron::3xflag::STOP::SL2::SV40::degron::wrmScarlet::egl-13NLS]) unc-119(ed3)* (Venz *et al.* 2021), and TJ356 *daf-16p::daf-16::GFP* (Henderson and Johnson 2001) were obtained from the Caenorhabditis Genetics Center (CGC).

shc-3 reporter strain

The translational *shc-3p::shc-3::GFP* fusion was generated by fusing a genomic DNA fragment containing 3.5 kb of sequence 5′ to the *shc-3* start codon, and sequences from exon 1 to the BglII site in exon 4 in-frame with the remaining *shc-3* cDNA. The *shc-3* genomic fragment was amplified with primers AATAAGCTTCTCGAGAAAGGCGCGCCCacacatacattcgaagaggcc and GTGCGAGATCTggttatcctatatcttccg. A GA linker (GAGAGAG) was added and both fragments were inserted in frame with GFP into the HindIII and MscI sites of the fire lab vector pPD95_77. This construct was injected into N2 animals at 25 ng/µL with 75 ng/µL *rol-6(su1006)* to generate *ltmEx10* or with 75 ng/µL 1 kb ladder DNA as a carrier to generate *ltmEx12*. Animals were anesthetized with levamisole, mounted on 1% agarose pads and examined on a Nikon Eclipse II microscope. Five independent lines from two separate injections were examined, all lines produced the same expression pattern. The *shc-3p::shc-3R145Q::GFP* reporter was generated using Q5 mutagenesis (NEB) with the wild-type reporter as template. This reporter was injected with 75 ng/µL of the dominant *rol-6(su1006)* marker to generate *ltmEx11[shc-3p::shc-3R145Q::GFP + rol-6(su1006)]*. Sequences and gene predictions used for the design of reporters were retrieved from Wormbase (Harris *et al.* 2020).

Pathogen assays

C. elegans slow killing assays were performed as previously described (Tan *et al.* 1999). Approximately 80–100 early adult animals were transferred to lawns of *Pseudomonas aeruginosa* PAO1 and an *Escherichia coli* OP50 control grown on 6 cm Slow-killing Media plates supplemented with 150 µM fluorodeoxyuridine (FUDR) to prevent egg-laying. Plates were incubated at 25 °C and scored for live worms daily. Animals unresponsive to touch with a platinum wire were considered dead and removed from the plate. Survival curves were generated using GraphPad Prism Software Version 9.2.0. statistical significance between treatment conditions was determined using the Log-rank (Mantel–Cox) test. To examine *ltmEx12* [*shc-3p::shc-3::GFP*] expression in response to PAO1, worms were grown to L4 and then transferred to lawns of either *E. coli* OP50 or *P. aeruginosa* PAO1, incubated for 24 h at 20 °C and photographed.

Survival assays

Eggs were collected by hypochlorite treatment of densely grown, but not starved, populations. Eggs were washed four times in M9 buffer and resuspended at 2 worms/µL in 7 mL M9 buffer at 20 °C. Worms were allowed to hatch overnight and hatched L1s were counted the following day. An aliquot was used to count live and dead worms. Each sample was counted daily in triplicate and survival curves were generated in GraphPad Prism. Survival assays were repeated at least three times.

Stress response

$CuSO_4$ sensitivity was assessed as described (Neumann-Haefelin *et al.* 2008). Briefly, 50–100 eggs were placed on NGM containing 40 µM $CuSO_4$ and incubated at 20 °C. The number of adult animals present after 4 d of growth was determined. Tunicamycin sensitivity was determined in the same way using 1 µg/mL Tunicamycin.

To test oxidative stress sensitivity, animals were allowed to develop until the population was a mix of L4 and young adult animals. Animals were then washed off with M9 and transferred to NGM plates supplemented with 4 mM paraquat and 100 µM FUDR. Animals were gently prodded with a platinum wire, unresponsive worms were scored as dead. Worms that crawled off the plate were censored. Statistical analysis was performed using GraphPad Prism, *P*-values were determined using a Mantel–Cox log-rank test. All assays were carried out in triplicate.

To monitor DAF-16::GFP nuclear entry, animals were incubated for 20 min at 37 °C and examined immediately. To examine nuclear export, animals were incubated for 1 h at 37 °C, at which time GFP was nuclear in most, if not all animals, worms were then transferred to 25 °C and examined 1.5 h after heat shock. Worms were scored as having DAF-16::GFP mostly nuclear, mostly cytoplasmic, or both nuclear and cytoplasmic (Oh *et al.* 2005). All experiments were repeated in at least three independent trials.

Heat sensitivity was tested by placing adult worms at 37 °C and scoring live and dead animals after 6 h. Survival was scored in triplicate. For rescue experiments, *ltmEx12* [*shc-3p::shc-3::GFP*] was crossed into *shc-3Δ* mutants. GFP-positive and -negative animals were scored on the same plates, with three plates per trial and in three independent trials. A paired *t*-test was used to verify the significance of rescue, comparing survival between paired GFP-positive and -negative samples.

Auxin-induced degradation of DAF-2

To observed SHC-3::GFP localization in response to auxin-induced DAF-2 degradation, *ltmEx12* [*shc-3p::shc-3::GFP*] was introduced into RAF2181 ieSi57 *daf-2(bch-40[degron::3xflag::STOP::SL2::SV40::degron::wrmScarlet::egl-13NLS])* (Venz *et al.* 2021) by mating. To verify the effectiveness of the auxin treatment, eggs were placed on 1 mM auxin-containing plates and on NGM plates (for later use). Auxin exposure induced developmental arrest in 100% of the animals, which validated the strain and the auxin-induced degradation of DAF-2. To test the impact of DAF-2 degradation on SHC-3::GFP localization, L4 GFP positive animals were transferred

to NMG media containing 1 mM auxin or control plates. Animals were grown at 20 °C for 24 h before imaging.

Results

K11E4.2 encodes a SHC-family protein

By examining SH2 domain-containing proteins in *C. elegans*, we identified a previously uncharacterized Shc family protein, K11E4.2/SHC-3. This protein contains the characteristic Shc-family domain structure, an N-terminal PTB domain and a C-terminal SH2 domain (Fig. 1a). SHC-3 was not previously identified as a SHC protein because the N-terminal domain was annotated as a PH-superfamily domain rather than a PTB domain. PH domains share the same basic structural fold as PTB domains but differ in function in that PH domains interact with phospholipids, while PTB domains bind phosphotyrosine-containing motifs. Intriguingly, the mammalian ShcA PTB domain can interact with both phosphotyrosine and phospholipid (Ravichandran *et al.* 1997), a feature that may explain sequence similarity of the Shc PTB domain and PH domains.

PTB domains are variable at the amino acid level. Based on specific structural features, they can be categorized as Shc-like, IRS-like, or Dab-like (Zhou *et al.* 1995; Eck *et al.* 1996; Farooq *et al.* 1999; Yun *et al.* 2003; Uhlik *et al.* 2005). K11E4.2 has features of the Shc PTB domain, including the conserved Arginine (R175 in hShcA, R145 in SHC-3) required for phosphotyrosine binding, an elongated loop between the PTB β1 and α2 that is distinct from Dab-like PTB domains, and the "Shc loop", an approximately 20 amino acid loop between α2 and β2 that is absent in IRS1 and DAB PTB domains (Zhou *et al.* 1995; Eck *et al.* 1996) (Fig. 1b, Supplementary Figs. 1 and 2). These structural features are conserved across *Caenorhabditis* K11E4.2 orthologs, supporting the identification of the N-terminal domain of K11E4.2 as a Shc-like PTB domain (Supplementary Fig. 1).

A second phosphotyrosine binding domain, the SH2 domain, lies at the C-terminus of Shc proteins. The N-terminus of the SH2 domain mediates its binding to phosphotyrosine motifs, this region in K11E4.2 is similar to human Shc proteins and the conserved arginine residue required for SH2 domains to bind phosphotyrosine is present in all *Caenorhabditis* SHC-3 sequences examined (Fig. 1c and Supplementary Fig. 1). The Alphafold predicted structure for SHC-3 (Jumper *et al.* 2021) overlaps well with the N-terminus of the solved ShcA SH2 domain structure (Supplementary Fig. 2). By contrast, the C-terminus of the SHC-3 SH2 domain is more divergent. Based on sequence alignment and the Alphafold prediction, the βE-βF region is likely absent or shortened relative to the human Shc proteins, however, Alphafold predictions are not experimentally validated and structural data for SHC-3 would be needed to verify this prediction (Terwilliger *et al.* 2024) (Supplementary Fig. 1). Variability in the C-terminus is common in the SH2 domain family, with deletions and insertions primarily found in the βE-βF and βG loop regions (Kaneko *et al.* 2012). The C-terminus of the *C. elegans* SHC-2 SH2 domain is also divergent, with insertions observed in these regions. Together, this may suggest that the *C. elegans* SHC-1 and SHC-3 SH2 domains have different binding specificities or may be differentially regulated through protein–protein interaction or posttranslational modification.

One of the most well-characterized functions of mammalian ShcA is the recruitment of Grb2 and associated proteins to tyrosine-phosphorylated transmembrane receptors resulting in the activation of the MAPK pathway. Grb2 binds ShcA through phosphorylated YXN motifs in the CH1 domain of Shc (Rozakis-Adcock *et al.* 1992). Similar to *C. elegans* SHC-1 and SHC-2, SHC-3 has little sequence similarity to mammalian Shc proteins in the CH1 domain and lacks the YXN motifs that serve as docking sites for GRB2 in mammalian ShcA, suggesting that, like *C. elegans* SHC-1, SHC-3 does not physically associate with SEM-5/Grb2.

### SHC-3 is expressed in the intestine

To examine SHC-3 expression and localization, we generated a SHC-3-GFP translational reporter (*shc-3p::shc-3::GFP*) (Fig. 3a). In contrast to *shc-1*, which is widely expressed (Neumann-Haefelin *et al.* 2008), *shc-3p::shc-3::GFP* expression was restricted to the intestine (Fig. 2). Expression was observed from embryogenesis through larval development and into the adult stage. Subcellular localization of SHC-3::GFP was temperature-dependent, with more SHC-3 localized to the apical membrane at higher temperatures and more cytoplasmic SHC-3 at lower temperatures (Fig. 2, a and b). Although both Shc proteins are expressed in the intestine, their subcellular localization is distinct. SHC-1 is strongly localized to the nucleus (Neumann-Haefelin *et al.* 2008), suggesting that the two proteins play distinct roles. The concentration of SHC-3, but not SHC-1 at the cell membrane may suggest that SHC-3 performs the more well-recognized role of Shc proteins, to function as an adapter for receptor tyrosine kinases.

Mammalian Shc proteins can be recruited to the plasma membrane through the interaction of the PTB domain with tyrosine-phosphorylated transmembrane proteins or membrane-associated proteins (Ravichandran *et al.* 1997). We reasoned that the inability to bind phosphotyrosine motifs might change the subcellular localization of SHC-3. To test this, we generated a *shc-3* translational fusion carrying a substitution of the conserved arginine (R145Q); the analogous substitution in human ShcA prevents phosphotyrosine binding and reduces membrane localization (Ravichandran *et al.* 1997). Apical localization was decreased for SHC-3R154Q::GFP relative to the wild-type protein, suggesting that, as with ShcA, the PTB domain, likely through phosphotyrosine binding, recruits SHC-3 to the membrane (Fig. 2c).

C. elegans Shc proteins function in stress response

To examine the function of *shc-3*, we generated a deletion allele that removes most of exons 1–4, we refer to this allele as *shc-3Δ* (Supplementary Fig. 3a). We obtained two additional alleles, *gk890887* and *gk466377*, from the million mutation project (Thompson *et al.* 2013). The *gk890887* allele produces an early stop (Q39*), while the *gk466377* allele produces the same R145Q substitution that reduces membrane localization in our transgenic animals (Supplementary Fig. 3b). All three mutants appeared superficially wild type in standard growth conditions. We measured reproduction and lifespan in *shc-3Δ* mutant animals. On an *E. coli* OP50 diet, *shc-3* mutants developed normally and produced wild-type brood sizes (Fig. 3a). Unlike *shc-1* mutants, *shc-3Δ* or *shc-3Q39** mutants did not have reduced lifespans. Further, *shc-3Δ* suppressed the shortened lifespan of *shc-1(ok198)* mutants (Fig. 3b), suggesting that the two proteins may have opposing functions.

The importance of Shc proteins in stress response is conserved in *C. elegans*. Loss of *shc-1* increases sensitivity to oxidative stress, copper sulfate, tunicamycin, heat, and pathogen exposure (Mizuno *et al.* 2008; Neumann-Haefelin *et al.* 2008). We asked whether *shc-3* was also required for response to these stresses. *Shc-3Δ* animals were not more sensitive to oxidative stress induced by paraquat, and, similar to what we observed with lifespan, loss of *shc-3* suppressed the sensitivity of *shc-1(ok198)* mutants (Fig. 3c). Increased sensitivity to $CuSO_4$ or tunicamycin
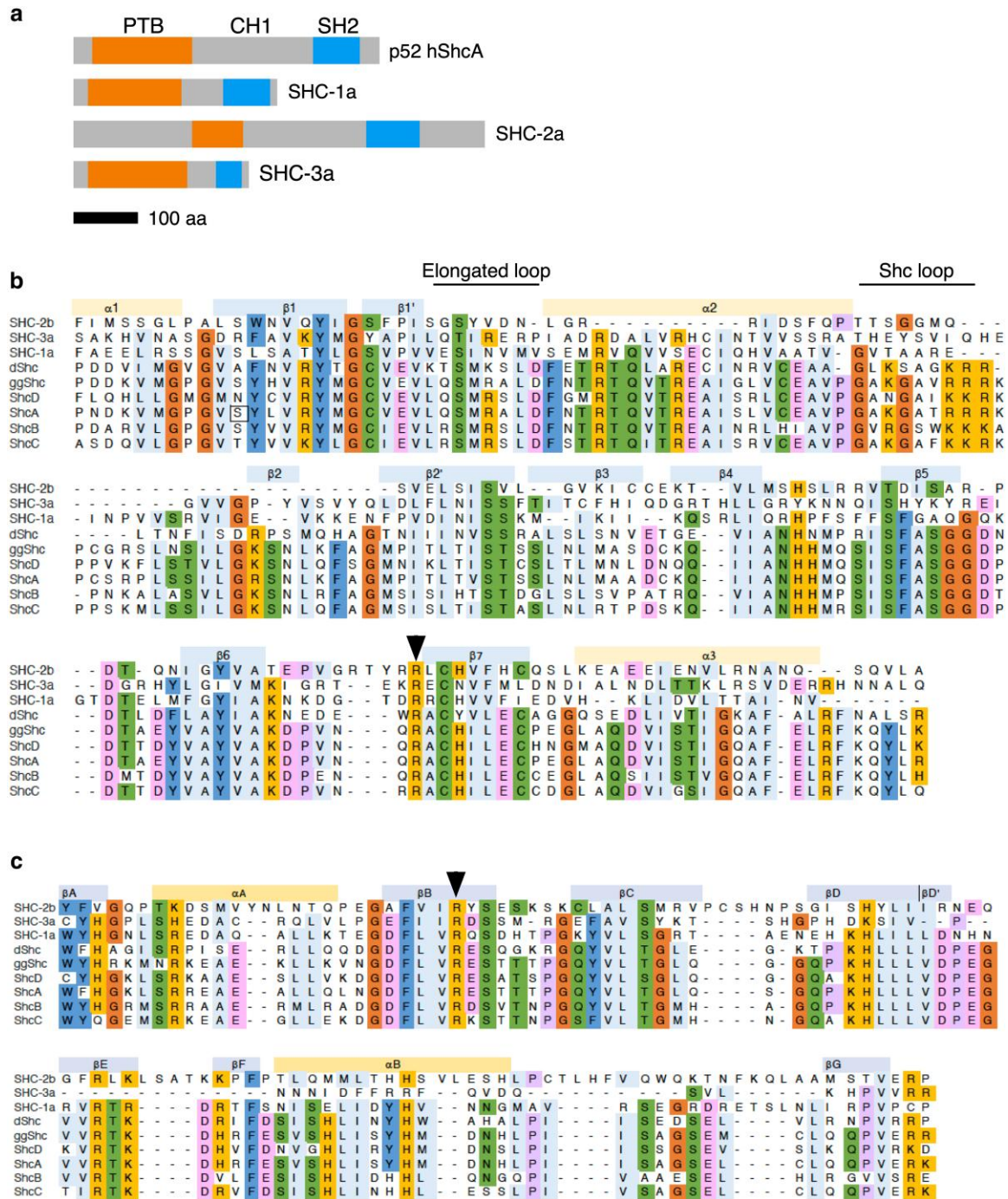
Fig. 1. K11E4.2 encodes a Shc-like protein. a) Domain organization of *C. elegans* SHC proteins relative to the human p52 isoform of human ShcA. The isoforms that produce the largest form of the proteins are shown (here isoform "a" for all). Location of *shc-3(syb1634)* deletion and amino acid substitutions in *shc-3(gk890887)* and *shc-3 (gk466377)* alleles are shown. b) Alignment of *C. elegans*, *Drosophila melanogaster* (d), *Galus galus* (gg) and Human (h) Shc PTB domains. Structural features of human ShcA are shown above the alignment. The elongated loop and the Shc loop, characteristic of Shc proteins are indicated. Arrowhead highlights the conserved arginine required for phosphotyrosine binding. c) Alignment of Shc SH2 domains. Arrowhead indicates conserved arginine required for phosphotyrosine binding.

was observed in *shc-1(ok198)* mutants but not in the two strong alleles of *shc-3* tested (Fig. 3, d and e). Loss of *shc-3* did not enhance or suppress sensitivity to CuSO₄, or tunicamycin in *shc-1(ok198)* mutants. However, these effects are likely mediated through the hypodermis where only *shc-1* is expressed. *Shc-1* expression in the hypodermis is sufficient to rescue the CuSO₄ sensitivity of *shc-1* mutants (Mizuno *et al.* 2008). Similarly, the tunicamycin sensitivity of *kgb-1* mutants is partially rescued by expression in the

hypodermis or muscle but not by intestinal expression of *kgb-1*. As SHC-1 functions upstream of KGB-1, it is likely that loss of SHC-1 in the hypodermis or muscle is responsible for the sensitivity to tunicamycin (Liu *et al.* 2018).

We next examined heat sensitivity in shc mutants. After 6 h at 37 °C, viability of *shc-1(ok198)* and *shc-3Δ* mutants was significantly reduced relative to N2 (Fig. 3f). While approximately 50% of wild-type animals survived at this time point, fewer than 20% survived
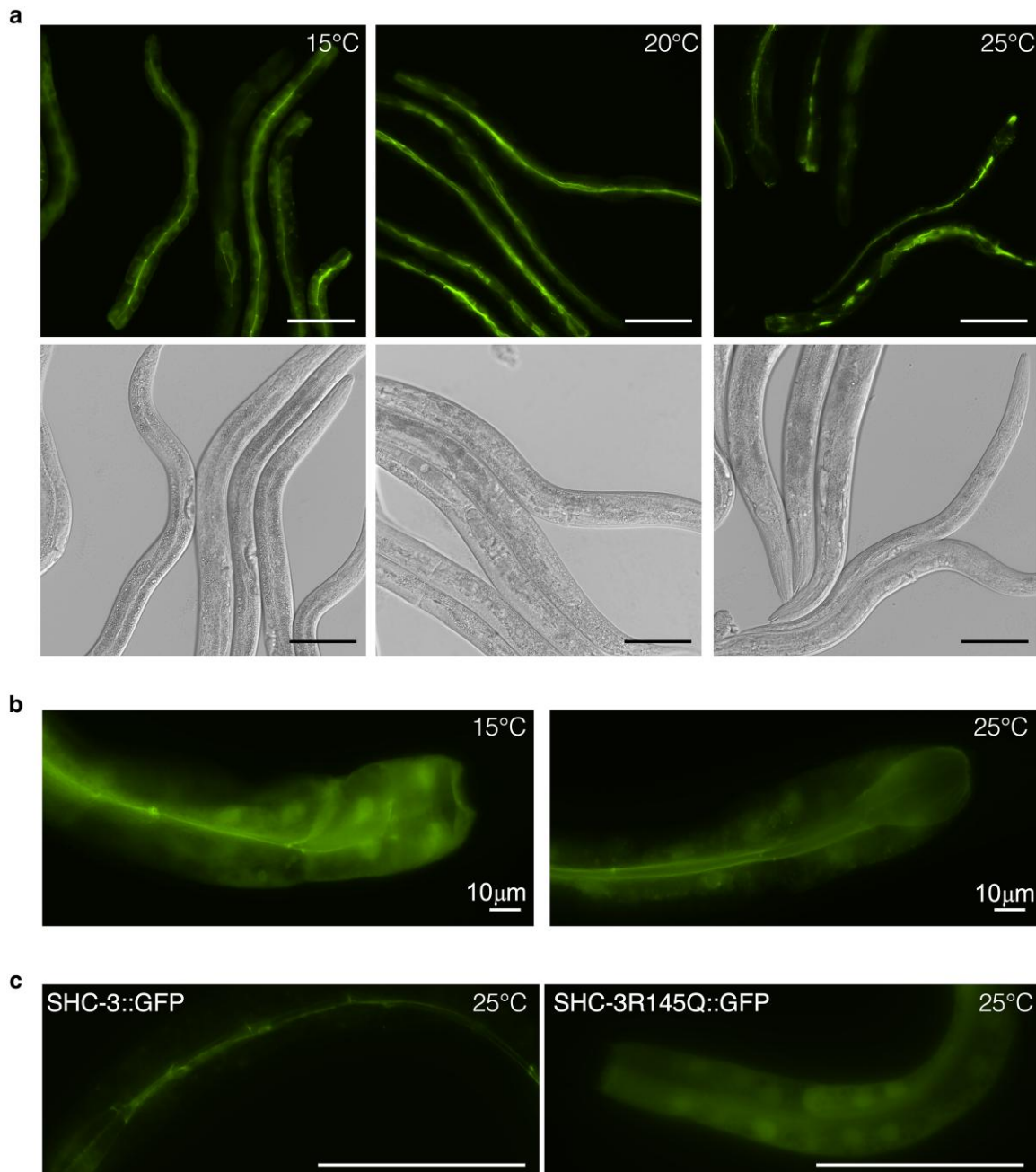
Fig. 2. *shc-3* is expressed in the intestine. a) Intestinal expression of *ltmEx12* [*shc-3p::shc-3::GFP*] at indicated temperatures in late L4 and early adult animals. SHC-3::GFP is localized to the cytoplasm and to the apical membrane. At lower temperatures (15 °C), SHC-3::GFP is enriched in the cytoplasm, while at higher temperatures (25 °C), more SHC-3 is localized to the membrane (b) *shc-3p::shc-3::GFP* expression in the anterior intestine at 25 or 15 °C (c) Substitution of the conserved arginine (R145Q) in the SHC-3 PTB domain reduces localization of SHC-3 to the plasma membrane. Animals are adults grown at 25 °C. *ltmEx10* [*shc-3p::shc-3::GFP + rol-6(su1006)*] (left) and *ltmEx11* [*shc-3p::shc-3R145Q::GFP + rol-6(su1006)*] (right) are shown. Scale bar = 100 μm, unless otherwise indicated.

for each of the *shc* mutants. Intriguingly, the loss of both *shc-1* and *shc-3* suppressed heat-sensitivity. To verify the role of *shc-3* in heat stress, we rescued *shc-3Δ* mutants with the *shc-3p::shc-3::GFP* transgene. Because this transgene is not integrated, we were able to score rescued and nonrescued animals in the same population based on the presence or absence of GFP. After 6 h at 37 °C, we observed increased viability of GFP-positive animals relative to GFP-negative animals demonstrating that expression of SHC-3::GFP rescued heat sensitivity in *shc-3Δ* mutants (Fig. 3g). In addition, shifting animals from 15 to 37°C promoted redistribution of SHC-3::GFP to the apical membrane (Fig. 3h).

Similar to what has been reported for *shc-1(ok198)* mutants, *shc-3Δ* mutants had increased vulnerability to infection by *Pseudomonas aeruginosa* PAO1. When exposed to PAO1, survival was significantly decreased in *shc-3Δ* mutants relative to wild-type animals (Fig. 4a). Further, in response to PAO1, SHC-3::GFP localization was increased at the apical membrane, suggesting that it functions in stress response at the membrane (Fig. 4b).

Shc-3 is required for long-term survival in L1 arrest

Shc-1 mutants develop a gonad dysmorphology phenotype following prolonged starvation, suggesting that SHC-1 is required for
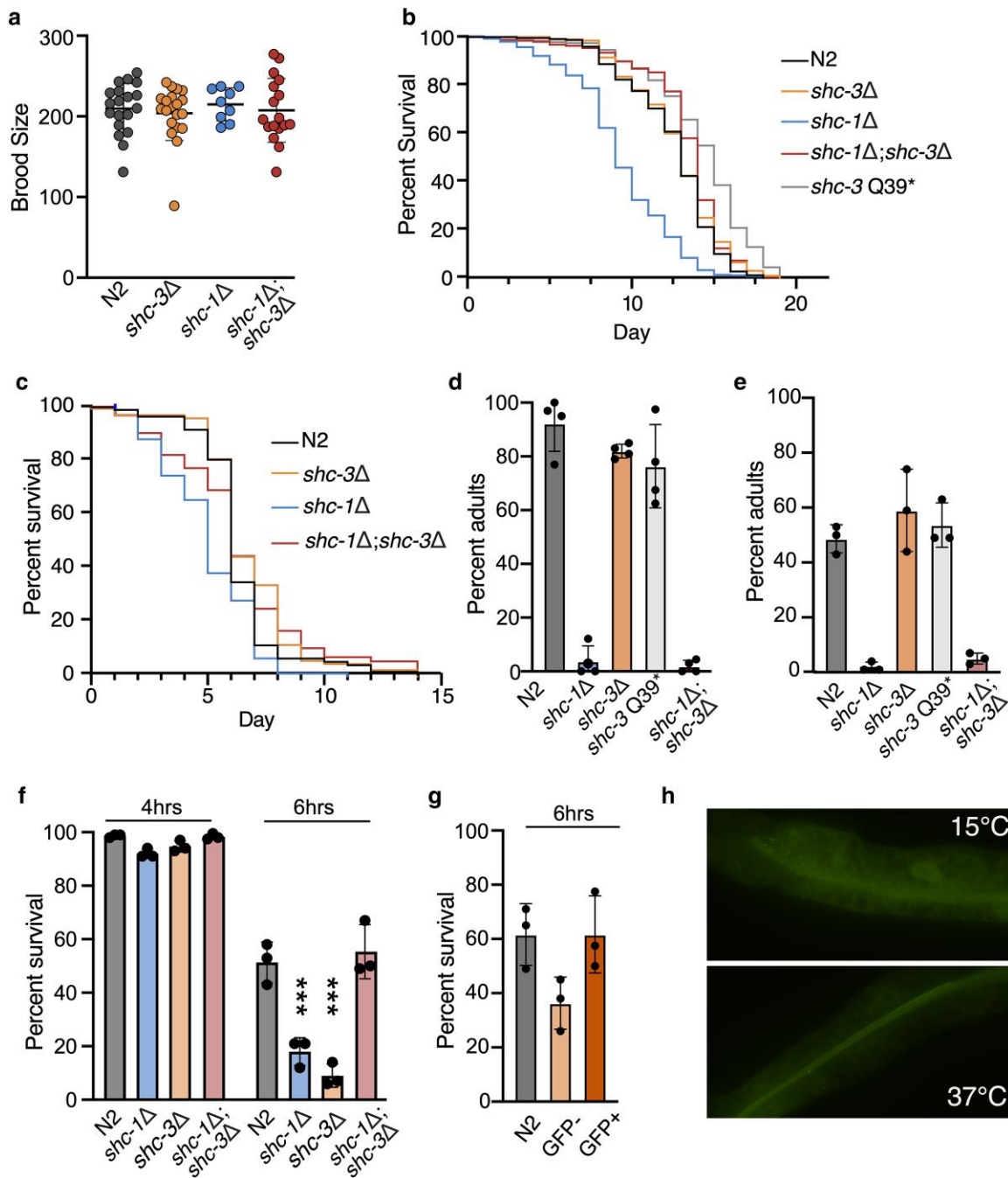
Fig. 3. Characterization of *shc-3* mutants. a) Total brood size of indicated mutants, N2 is used as wild-type, *shc-3Δ* refers to *shc-3(syb1634)*, *shc-3* R145Q refers to *shc-3(gk466377)* and *shc-3Q38** refers to *shc-3(gk890887)*. Individual points represent brood size of an individual animal. Mean and standard deviation are shown. b) Lifespan of Shc mutants. Days indicates days of adulthood. As previously shown, *shc-1(ok198)* mutants have shortened lifespans ($P < 0.005$). *shc-3* mutation did not decrease lifespan, relative to N2, but *shc-3Δ* mutants suppressed the shortened lifespan of *shc-1(ok198)* mutants ($P < 0.005$). Significance was calculated by Mantel–Cox test with Bonferroni correction for multiple hypothesis testing. c) Survival following exposure of adult animals to 4 μm paraquat. Increased sensitivity of *shc-1* mutants is suppressed by *shc-3* mutation ($P < 0.005$ Wilcoxon test with Bonferroni correction). d) Development to adults of indicated mutants after exposure to 40 μM $CuSO_4$. (e) Development to adults after exposure to tunicamycin. f) Survival of animals in response to 37 °C heat shock at 4 and 6 h is shown. All genotypes were scored in triplicate with >100 animals per sample, trials are plotted with mean and standard deviation. ***$P < 0.001$ one way ANOVA with Dunnett's multiple comparison test. g) Rescue of *shc-3Δ* heat shock sensitivity with *ltmEx12 [shc-3p::shc-3::GFP]* transgene, GFP positive and negative animals were scored on the same plates, with 6-h heat shock. $P < 0.05$ paired *t*-test. h) *ltmEx12 [shc-3p::shc-3::GFP]* expression in adults animals maintained at 15 °C (top) compared to animals incubated at 37 °C for 1 h (bottom).

recovery from starvation (Wolf *et al.* 2014). It may also play a role in recovery from long-term arrest through KGB-1, given that *kgb-1* mutants arrested for long periods in L1 are slow to recover from arrest and have decreased lifespans (Roux *et al.* 2016, 2022). We examined the survival of Shc mutants after prolonged L1 arrest.

Survival of *shc-1(ok198)* and all three *shc-3* mutants was decreased relative to wild-type animals (Fig. 5a). The decreased survival of *shc-3* R145Q suggests that the PTB domain is important for this function. While mutants in both Shc genes displayed the same phenotype, no enhancement of this effect was observed when
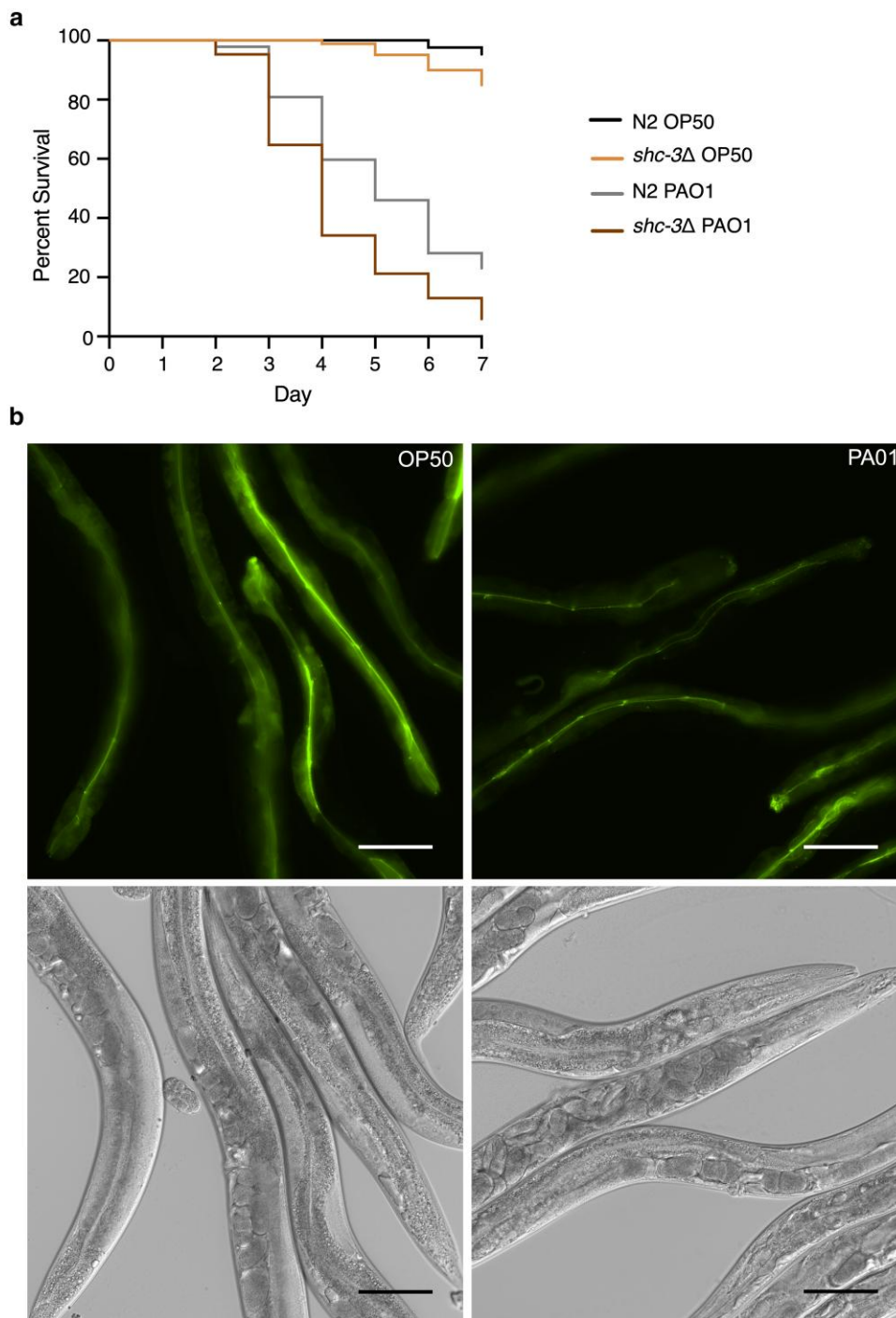
Fig. 4. *shc-3* mutants have increased susceptibility to pathogen infection. a) Survival following exposure to *P. aeruginosa* is decreased in *shc-3Δ* mutants ($P < 0.0002$ log-rank test). Median survival of *shc-3Δ* mutants is approximately one day less than wild-type animals. b) Expression of SHC-3::GFP in response to *E. coli* OP50 or *P. aeruginosa* PAO1. Adult animals carrying *ltmEx12 [shc-3p::shc-3::GFP]* exposed for 24 h at 20 °C are shown. Scale bar is 100μm.

both genes were lost (Fig. 5b). Surprisingly, *shc-3; shc-1* double mutants had improved survival relative to *shc-1* mutants alone, suggesting that SHC-1 and SHC-3 do not act redundantly but that they do act in the same pathway to regulate survival in L1 arrest.

To verify the role of *shc-3* in L1 arrest, we introduced the *shc-3p::shc-3::GFP* reporter into *shc-3Δ* animals to determine whether it could rescue the decreased survival of worms in L1 arrest. Because we could not determine GFP status in dead animals, we examined instead the fraction of live GFP animals in the population over time. Our rationale was that rescue would result in an increase in the ratio of GFP-positive (SHC-3+) to GFP-negative (*shc-3Δ*) animals over time. Indeed, this is what we observed; the ratio remained relatively constant until approximately day 12, after which we observed a gradual increase in the ratio of GFP-positive to GFP-negative animals (overall slope 2.5, $P < 0.0001$) (Fig. 5c). The timing of this increase is consistent with the timing of decreased L1 survival in *shc-3* mutants. In the first 12–14 days there is little difference in survival between wild-type and *shc-3Δ* mutant animals. It is only after this period that the decreased survival of *shc-3Δ* animals becomes evident (Fig. 5a).
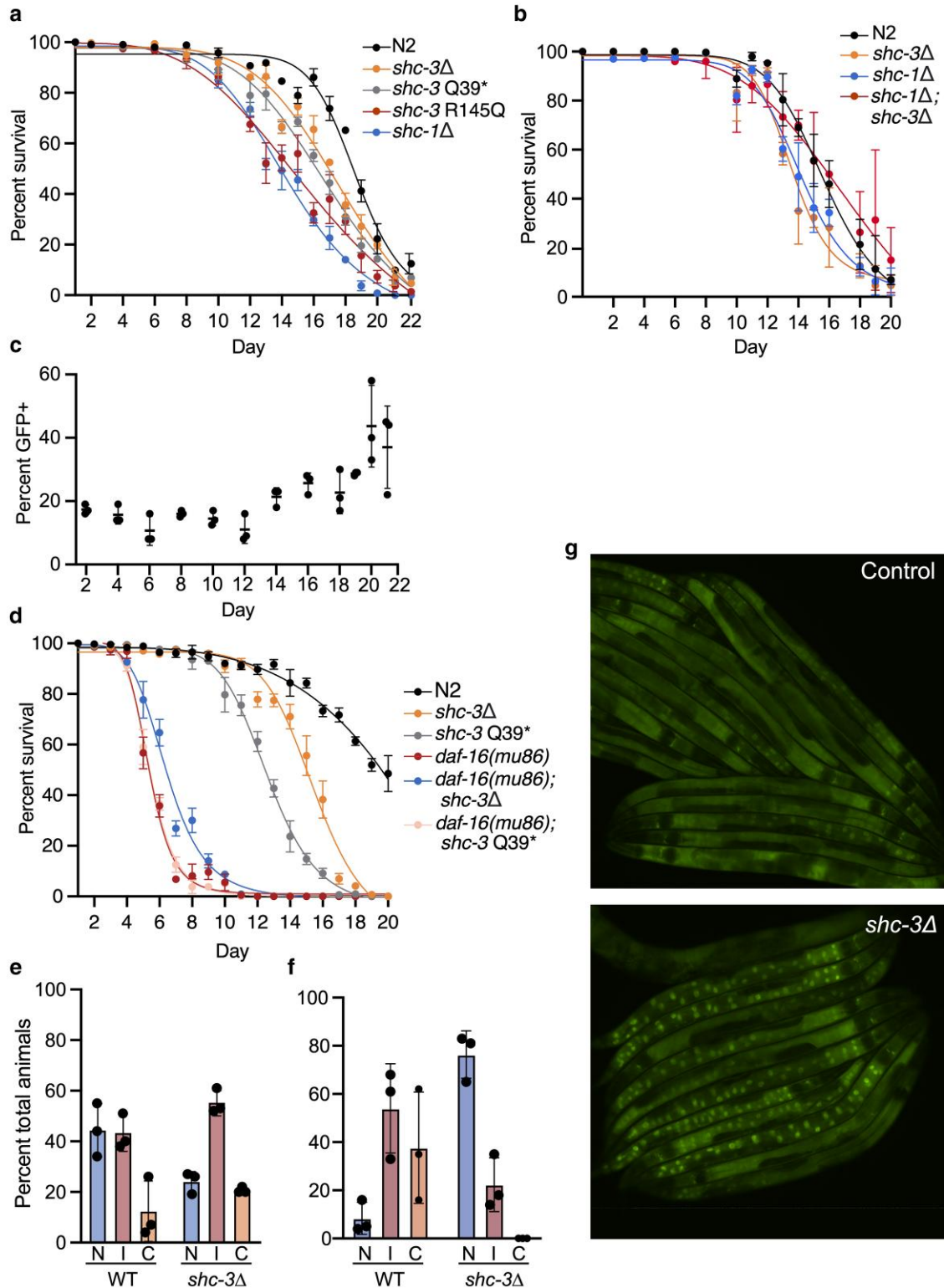
Fig. 5. *shc-3* is required for long-term survival in L1 arrest. a) *shc-1* and *shc-3* mutants have reduced survival in L1 arrest relative to N2 animals. The mean and standard deviation of three replicates is shown. b) Reduced survival of *shc-1* and *shc-3* mutants was not further enhanced in double mutants (data as in a). c) Rescue of *shc-3Δ* L1 survival defect. In a population of *shc-3Δ ; ltmEx12 [shc-3p::shc-3::GFP]* animals arrested in L1, the proportion of GFP-positive animals increases over time. d) *shc-3* mutation does not enhance the reduced survival of *daf-16 (mu86)* mutants. Animals were scored in triplicate at each time point. Mean and standard deviation are shown. e) Wild-type and *shc-3Δ* animals expressing DAF-16::GFP were categorized as having mostly nuclear (N), intermediate (I), or mostly cytoplasmic (C) localization of DAF-16::GFP immediately following a 20 min heat shock. f) DAF-16 nuclear exit was measured in adult animals following a 1 h heat shock and 1.5 h recovery period. Animals were categorized as in (e). For (a) to (d) and (b), each point represents a population of at least 30 animals. Heat shock was carried out in triplicate. g) Delayed DAF-16::GFP nuclear exit following recovery from heat shock (as in f).

IIS is a key regulator of survival during L1 arrest in *C. elegans* (Baugh and Sternberg 2006). Loss of the insulin-like receptor *daf-2* or of the PI3K subunit *age-1* increases survival in L1 arrest, while loss of their downstream target FOXO/*daf-16* decreases survival (Muñoz and Riddle 2003; Baugh and Sternberg 2006; Zhang *et al.* 2011). Two functions have been proposed for SHC-1, as a physical interactor and negative regulator of the insulin-like receptor DAF-2, and as an activator of JNK signaling; both functions converge on DAF-16 (Neumann-Haefelin *et al.* 2008). To determine if SHC-3 influences L1 arrest via the IIS pathway, we measured survival in L1 arrest of *daf-16* mutants carrying *shc-3Δ* or *shc-3 Q39** mutations and found that neither allele decreased survival of *daf-16* mutants, suggesting that SHC-3 and DAF-16 function in the same pathway to regulate survival in L1 arrest (Fig. 5d). The similarity of phenotypes between *daf-16* and *shc-3* mutants would suggest that in L1 arrest SHC-3 and SHC-1 function as positive regulators of DAF-16, and therefore negative regulators of IIS.

SHC-3 regulates DAF-16 nuclear entry and exit

To further understand the relationship between SHC-3 and insulin signaling, we examined the influence of *shc-3* mutation on DAF-16 nuclear localization during stress. Activation of IIS prevents DAF-16 from entering the nucleus and activating its transcriptional targets. Localization of DAF-16::GFP can therefore serve as a proxy for insulin signaling (Henderson and Johnson 2001). In response to a 20 min heat shock, DAF-16::GFP nuclear localization was decreased in *shc-3* mutant animals relative to wild-type controls, again suggesting that SHC-3 is a positive regulator of DAF-16 (Fig. 5e). We also examined recovery from heat shock by inducing complete nuclear localization with a long heat shock followed by a 1.5 h recovery period at 20 °C. Under these conditions, more DAF-16::GFP was observed in the nucleus of *shc-3* mutants than controls, suggesting that recovery from heat shock is slowed in these animals (Fig. 5, f and g). The delayed nuclear entry and exit of DAF-16 in *shc-3* mutants suggests that SHC-3 may be required to mediate rapid changes in insulin signaling.

DAF-2 has three NPXY/NXXY motifs that could potentially bind the SHC-3 PTB domain and bring SHC-3 to the membrane. To determine whether DAF-2 was required to recruit SHC-3 to the membrane, we used a degron-tagged allele of *daf-2*, *daf-2(bch40)* (Venz *et al.* 2021) and examined the localization of SHC-3::GFP following auxin-induced degradation of DAF-2. In adult animals, 24 h exposure to auxin decreased the intensity of SHC-3::GFP at the cell membrane, but did not result in a complete loss of apical membrane localization (Fig. 6a). To show that auxin was effective in these animals, we placed L1 animals on auxin and monitored development. As previously reported (Venz *et al.* 2021), developmental arrest occurred in these animals, but not in L1, demonstrating that auxin was effective in inducing DAF-2 degradation but that it likely produces a strong loss of function, but not a null phenotype (Fig. 6b). Although we cannot exclude the possibility that an incomplete loss of DAF-2 protein allows some SHC-3 to remain at the membrane, our observations could also be explained if DAF-2 regulates membrane localization of SHC-3 indirectly or if other binding partners also bring SHC-3 to the membrane.

Discussion

Many regulators influence the localization and activity of DAF-16, together determining the timing and extent of IIS. We characterized a previously unidentified *C. elegans* Shc gene, *shc-3*, and found

that it functions in the IIS pathway to regulate survival in L1 arrest and response to heat stress. Unlike other mediators of IIS, SHC-3 is not widely expressed. This, together with the fact that the mutant phenotypes observed are less severe than those of other IIS pathway mutants, demonstrates that SHC-3 is not absolutely required for insulin signaling. Instead, SHC-3 may modify insulin signaling in the intestine to accommodate gut-specific functions or requirements.

SHC-3 localization during heat stress and pathogen exposure suggests that SHC-3 functions at the membrane to modify signaling. The cytoplasmic localization observed at 15 °C suggests that SHC-3 requires an interaction partner to keep it at the membrane. Mammalian ShcA is recruited to the insulin-like growth factor receptor through interaction with a conserved phosphotyrosine motif. This motif is conserved in DAF-2 and likely acts to recruit PTB-domain-containing proteins, including IRS-1 and SHC-1, upon receptor activation. The localization of SHC-3 to the membrane at higher temperatures suggests that it is present at the membrane when DAF-16 is in the nucleus, suggesting SHC-3 may negatively regulate the DAF-2-AGE-1-AKT-1 pathway during heat stress. This may occur through competitive binding with other PTB-domain containing proteins that positively affect DAF-2 signaling, by recruiting other signaling interactors that modify DAF-2 signaling, or by influencing trafficking of the receptor.

Although genetic interactions show that both *shc-1* and *shc-3* influence the IIS pathway, they play different molecular roles. Mutations in either gene reduce survival in L1 arrest without enhancement of mutant phenotypes in double mutants, suggesting that the two proteins cannot substitute for one another. Interactions between *shc-1* and *shc-3* are difficult to summarize with a single model; in some cases, *shc-3* mutations suppress the effects of *shc-1* mutations, while in other cases, loss of either gene results in the same phenotype. Interpreting the role of SHC-1 in these interactions is challenging because in addition to functioning as a positive regulator of the MLK-1-MEK-1-KGB-1 pathway, SHC-1 binds DAF-2 (Neumann-Haefelin *et al.* 2008). Further, SHC-1 is widely expressed and cell nonautonomous functions may also affect DAF-16 signaling in the intestine. For example, noncell-autonomous regulation of DAF-16 nuclear localization in the intestine can be mediated by expression of KGB-1 in the nervous system (Liu *et al.* 2018). Interactions between DAF-16 and the KGB-1 pathway are complex; KGB-1 functions as a positive regulator of DAF-16 during development but as a negative regulator in adults (Twumasi-Boateng *et al.* 2012; Liu *et al.* 2018). As a regulator of KGB-1 signaling, SHC-1 is likely to function in the same capacity.

The ability of *shc-3* mutation to suppress oxidative stress sensitivity and shortened lifespan in *shc-1* mutants could result from the two proteins antagonizing one another. This antagonism could be explained if both SHC-1 and SHC-3 bind DAF-2, but subsequently recruit different mediators, a balance of which is required to generate a context-appropriate response. This is consistent with the ability of mammalian Shc proteins to bind to the same target proteins with different outcomes (Liu and Meakin 2002; Finetti *et al.* 2009; Patrussi *et al.* 2014). The balance of protein binding in these cases can fine-tune downstream signaling, providing high or low levels of signaling outputs that are context-appropriate. Alternatively, the outcome of *shc-1* and *shc-3* interactions could reflect the balance of positive and negative activities on DAF-16 and may be determined by which function of SHC-1 is involved and in which tissue.

DAF-16 nuclear import and export were slowed in *shc-3* mutants, which may suggest that in the absence of SHC-3, DAF-2
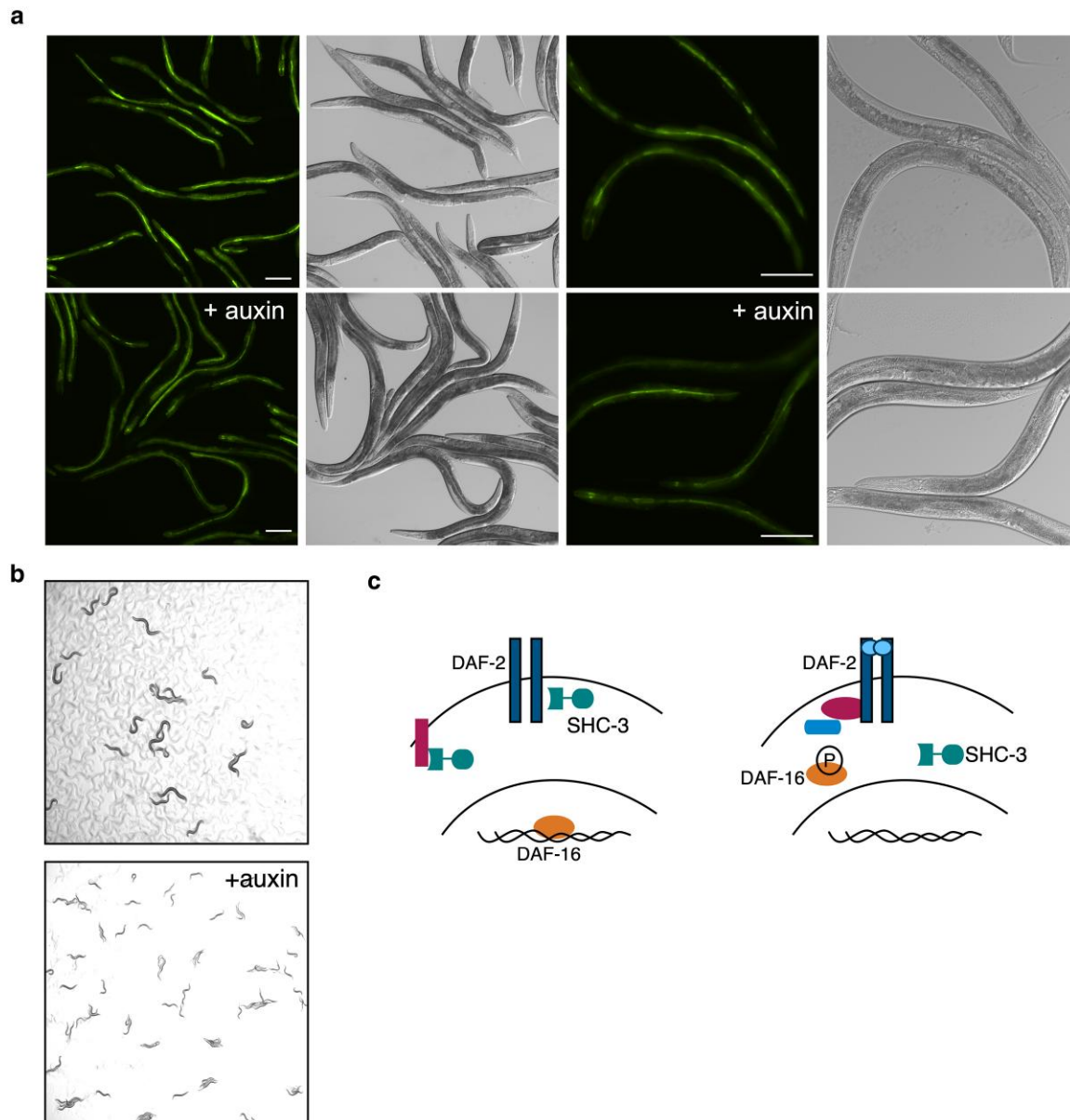
Fig. 6. Forced degradation of DAF-2 alters SHC-3::GFP expression. a) Expression of SHC-3::GFP in *ltmEx12* [*shc-3p::shc-3::GFP*]; ieSi57*daf-2*(*bch-40*[degron::3xflag::STOP::SL2::SV40::degron::wrmScarlet::*egl-13*NLS]) animals with and without the addition of auxin. b) Auxin-mediated degradation of DAF-2 induces developmental arrest. c) SHC-3 functions at the membrane, possibly through interaction with DAF-2, but may have additional binding partners.

signaling is slowed or less responsive to stimulus. The cumulative effects of SHC-3 loss would, therefore, depend on the activity of DAF-2 and other DAF-16 regulators. For example, if we assume that DAF-2 is active during development before reaching the L1 checkpoint, the loss of SHC-3 may reduce survival because DAF-16 entry into the nucleus is delayed upon starvation. Alternatively, if DAF-16 cycles between the nucleus and the cytoplasm, SHC-3 may alter the time it spends in each compartment, which could impact survival.

The ability of SHC-3 to enhance both nuclear entrance and exit of DAF-16::GFP suggests that it may function to promote rapid changes in insulin signaling. There are advantages to tailoring the speed of the DAF-16 response. In some conditions, rapid response may be favorable, for example in response to toxins and other stresses, when immediate mitigation is needed. By contrast, a slow response may be favored in cases where environmental changes fluctuate rapidly but where an immediate response is not beneficial. This slowing may act to dampen the response, preventing dramatic changes in signaling in the absence of a sustained stimulus. A more rapid response may be beneficial in the intestine, where exposure to pathogens and sub-optimal foods may require immediate response.

Data availability

Strains and plasmids are available upon request. All data are included in the manuscript and supplemental files. Supplementary Fig. 1 is an alignment of SHC-3 across Caenorhabditis species. Supplementary Fig. 2 is a comparison of human ShcA with the Alphafold predicted structure of SHC-3. Supplementary Fig. 3 is a description of the *shc-3* locus and all *shc-3* mutants used in this study. Supplementary Table 1 is a summary of survival data used in the study.

Supplemental material available at GENETICS online.

Acknowledgments

Funding

Conflicts of interest

The authors declare no conflict of interest.

Author contributions

MDB, VLLG, WRH, JS, and LM carried out experiments. All authors read and provided input on the manuscript.

Literature cited

Baugh LR, Sternberg PW. 2006. DAF-16/FOXO regulates transcription of *cki-1*/Cip/Kip and repression of *lin-4* during *C. elegans* L1 arrest. Curr Biol. 16(8):780–785. doi:10.1016/j.cub.2006.03.021.

Dogra D, Kulalert W, Schroeder FC, Kim DH. 2022. Neuronal KGB-1 JNK MAPK signaling regulates the dauer developmental decision in response to environmental stress in *Caenorhabditis elegans*. Genetics. 220(1):iyab186. http://dx.doi.org/10.1093/genetics/iyab186.

Eck MJ, Dhe-Paganon S, Trüb T, Nolte RT, Shoelson SE. 1996. Structure of the IRS-1 PTB domain bound to the juxtamembrane region of the insulin receptor. Cell. 85(5):695–705. doi:10.1016/s0092-8674(00)81236-2.

Farooq A, Plotnikova O, Zeng L, Zhou M-M. 1999. Phosphotyrosine binding domains of Shc and insulin receptor substrate 1 recognize the NPXpY motif in a thermodynamically distinct manner. J Biol Chem. 274(10):6114–6121. http://dx.doi.org/10.1074/jbc.274.10.6114.

Finetti F, Savino MT, Baldari CT. 2009. Positive and negative regulation of antigen receptor signaling by the Shc family of protein adapters. Immunol Rev. 232(1):115–134. doi:10.1111/j.1600-065X.2009.00826.x.

Harris TW, Arnaboldi V, Cain S, Chan J, Chen WJ, Cho J, Davis P, Gao S, Grove CA, Kishore R, *et al.* 2020. WormBase: a modern model organism information resource. Nucleic Acids Res. 48(D1): D762–D767. doi:10.1093/nar/gkz920.

Henderson ST, Johnson TE. 2001. *daf-16* integrates developmental and environmental inputs to mediate aging in the nematode *Caenorhabditis elegans*. Curr Biol. 11(24):1975–1980. doi:10.1016/s0960-9822(01)00594-2.

Hisamoto N, Nagamori Y, Shimizu T, Pastuhov SI, Matsumoto K. 2016. The *C. elegans* discoidin domain receptor DDR-2 modulates the met-like RTK-JNK signaling pathway in axon regeneration. PLoS Genet. 12(12):e1006475. doi:10.1371/journal.pgen.1006475.

Jumper J, Evans R, Pritzel A, Green T, Figurnov M, Ronneberger O, Tunyasuvunakool K, Bates R, Žídek A, Potapenko A, *et al.* 2021. Highly accurate protein structure prediction with AlphaFold. Nature. 596(7873):583–589. doi:10.1038/s41586-021-03819-2.

Kaneko T, Joshi R, Feller SM, Li SS. 2012. Phosphotyrosine recognition domains: the typical, the atypical and the versatile. Cell Commun Signal. 10(1):32. doi:10.1186/1478-811X-10-32.

Liu H-Y, Meakin SO. 2002. ShcB and ShcC activation by the Trk family of receptor tyrosine kinases. J Biol Chem. 277(29):26046–26056. doi:10.1074/jbc.M111659200.

Liu L, Ruediger C, Shapira M. 2018. Integration of stress signaling in *Caenorhabditis elegans* through cell-nonautonomous contributions of the JNK homolog KGB-1. Genetics. 210(4):1317–1328. doi:10.1534/genetics.118.301446.

Luzi L, Confalonieri S, Di Fiore PP, Pelicci PG. 2000. Evolution of Shc functions from nematode to human. Curr Opin Genet Dev. 10(6):668–674. doi:10.1016/s0959-437x(00)00146-5.

Mizuno T, Fujiki K, Sasakawa A, Hisamoto N, Matsumoto K. 2008. Role of the *Caenorhabditis elegans* Shc adaptor protein in the c-Jun N-terminal kinase signaling pathway. Mol Cell Biol. 28(23):7041–7049. doi:10.1128/MCB.00938-08.

Muñoz MJ, Riddle DL. Positive selection of Caenorhabditis elegans mutants with increased stress resistance and longevity. Genetics. 2003;163(1):171–180. doi:10.1093/genetics/163.1.171.

Neumann-Haefelin E, Qi W, Finkbeiner E, Walz G, Baumeister R, Hertweck M. 2008. SHC-1/p52Shc targets the insulin/IGF-1 and JNK signaling pathways to modulate life span and stress response in *C. elegans*. Genes Dev. 22(19):2721–2735. doi:10.1101/gad.478408.

Oh SW, Mukhopadhyay A, Svrzikapa N, Jiang F, Davis RJ, Tissenbaum HA. 2005. JNK regulates lifespan in *Caenorhabditis elegans* by modulating nuclear translocation of forkhead transcription factor/DAF-16. Proc Natl Acad Sci U S A. 102(12):4494–4499. doi:10.1073/pnas.0500749102.

Patrussi L, Capitani N, Cannizzaro E, Finetti F, Lucherini OM, Pelicci PG, Baldari CT. 2014. Negative regulation of chemokine receptor signaling and B-cell chemotaxis by p66Shc. Cell Death Dis. 5(2): e1068–e1068. http://dx.doi.org/10.1038/cddis.2014.44.

Ravichandran KS, Zhou MM, Pratt JC, Harlan JE, Walk SF, Fesik SW, Burakoff SJ. 1997. Evidence for a requirement for both phospholipid and phosphotyrosine binding via the Shc phosphotyrosine-binding domain in vivo. Mol Cell Biol. 17(9):5540–5549. doi:10.1128/MCB.17.9.5540.

Roux AE, Langhans K, Huynh W, Kenyon C. 2016. Reversible age-related phenotypes induced during larval quiescence in *C. elegans*. Cell Metab. 23(6):1113–1126. doi:10.1016/j.cmet.2016.05.024.

Roux AE, Zhang C, Paw J, Zavala-Solorio J, Malahias E, Vijay T, Kolumam G, Kenyon C, Kimmel JC. 2022. Diverse partial reprogramming strategies restore youthful gene expression and transiently suppress cell identity. Cell Syst. 13(7):574–587.e11. doi:10.1016/j.cels.2022.05.002.

Rozakis-Adcock M, McGlade J, Mbamalu G, Pelicci G, Daly R, Li W, Batzer A, Thomas S, Brugge J, Pelicci PG, *et al.* 1992. Association of the Shc and Grb2/Sem5 SH2-containing proteins is implicated in activation of the Ras pathway by tyrosine kinases. Nature. 360(6405):689–692. doi:10.1038/360689a0.

Stiernagle T. 2006. Maintenance of *C. elegans*, editors. The C. elegans Research Community, WormBook. (February 11, 2006). http://dx.doi.org/10.1895/wormbook.1.101.1.

Tan MW, Mahajan-Miklos S, Ausubel FM. 1999. Killing of Caenorhabditis elegans by Pseudomonas aeruginosa used to model mammalian bacterial pathogenesis. Proc Natl Acad Sci U S A. 96(2):715–720. doi:10.1073/pnas.96.2.715.

Terwilliger TC, Liebschner D, Croll TI, Williams CJ, McCoy AJ, Poon BK, Afonine PV, Oeffner RD, Richardson JS, Read RJ, *et al.* 2024. AlphaFold predictions are valuable hypotheses and accelerate but do not replace experimental structure determination. Nat Methods. 21(1):110–116. doi:10.1038/s41592-023-02087-4.

Thompson O, Edgley M, Strasbourger P, Flibotte S, Ewing B, Adair R, Au V, Chaudhry I, Fernando L, Hutter H, *et al.* 2013. The million mutation project: a new approach to genetics in *Caenorhabditis elegans*. Genome Res. 23(10):1749–1762. doi:10.1101/gr.157651.113.

Twumasi-Boateng K, Wang TW, Tsai L, Lee K-H, Salehpour A, Bhat S, Tan M-W, Shapira M. 2012. An age-dependent reversal in the protective capacities of JNK signaling shortens *Caenorhabditis elegans* lifespan. Aging Cell. 11(4):659–667. doi:10.1111/j.1474-9726.2012.00829.x.

Uhlik MT, Temple B, Bencharit S, Kimple AJ, Siderovski DP, Johnson GL. 2005. Structural and evolutionary division of phosphotyrosine binding (PTB) domains. J Mol Biol. 345(1):1–20. doi:10.1016/j.jmb.2004.10.038.

Venz R, Pekec T, Katic I, Ciosk R, Ewald CY. 2021. End-of-life targeted degradation of DAF-2 insulin/IGF-1 receptor promotes longevity free from growth-related pathologies. Elife. 10:e71335. doi:10.7554/eLife.71335.

Wolf T, Qi W, Schindler V, Runkel ED, Baumeister R. 2014. Doxycyclin ameliorates a starvation-induced germline tumor in *C. elegans daf-18*/PTEN mutant background. Exp Gerontol. 56:114–122. doi:10.1016/j.exger.2014.04.002.

Yun M, Keshvara L, Park C-G, Zhang Y-M, Dickerson JB, Zheng J, Rock CO, Curran T, Park H-W. 2003. Crystal structures of the Dab homology domains of mouse disabled 1 and 2. J Biol Chem. 278(38):36572–36581. doi:10.1074/jbc.M304384200.

Zhang X, Zabinsky R, Teng Y, Cui M, Han M. 2011. microRNAs play critical roles in the survival and recovery of *Caenorhabditis elegans* from starvation-induced L1 diapause. Proc Natl Acad Sci U S A. 108(44):17997–18002. doi:10.1073/pnas.1105982108.

Zhou M-M, Ravichandran KS, Olejniczak ET, Petros AM, Meadows RP, Sattler M, Harlan JE, Wade WS, Burakoff SJ, Fesik SW. 1995. Structure and ligand recognition of the phosphotyrosine binding domain of Shc. Nature. 378(6557):584–592. doi:10.1038/378584a0.

Editor: V. Reinke